

Original Article

Predictive value of diffusion-weighted magnetic resonance imaging for cervical lymph node metastasis in nasopharyngeal carcinoma after chemoradiotherapy

Ying Hu, Fengmei Zhou, Qingwu Wu, Jipeng Ren, Zheng Li, Xiaohuan Liu, Ruifang Yan, Dongming Han

Department of Medical Imaging, The First Affiliated Hospital of Xinxiang Medical University, Weihui 453100, P.R. China

Received October 14, 2015; Accepted April 8, 2016; Epub November 15, 2016; Published November 30, 2016

Abstract: Objective: Our aim is to investigate the predictive value of diffusion-weighted magnetic resonance imaging (DW-MRI) and apparent diffusion coefficient (ADC) values in cervical lymph node metastasis from nasopharyngeal carcinoma (NPC) after chemoradiotherapy. Methods: Between March 2010 and January 2013, 71 patients diagnosed with NPC were selected in our study. All patients received conventional magnetic resonance imaging (MRI) and diffusion-weighted imaging (DWI) examinations. The maximum cross-sectional area of metastatic lymph nodes was measured under sequence map of MRI, while the ADC value was measured under the selected region of interests (ROI) of ADC. Results: The maximum cross-sectional area of metastatic lymph nodes in both CR and non-CR group were retreated after chemotherapy compared with those before chemotherapy (all $P < 0.05$), and they all presented an obvious retreat after radiotherapy (all $P < 0.001$). The ADC value of metastatic lymph nodes after chemotherapy was evidently increased than those before chemotherapy ($t = 13.27$, $P < 0.001$), and it increased more significantly after radiotherapy ($t = 34.62$, $P < 0.001$). An obviously increasing trend was found in the mean ADC values of residual lymph nodes one month after treatment compared with those before treatment and no metastatic lymph nodes after treatment, which indicated a statistical significance (all $P < 0.001$). The sensitivity, specificity, positive predictive value, negative predictive value, accuracy and area under curve (AUC) after treatment of NPC were 0.905, 0.680, 0.763, 0.583, 0.732 and 0.816, respectively, predicting by the threshold value setting by mean ADC value before treatment (8.11×10^{-4} mm²/s). Conclusions: Our results demonstrated both DW-MRI and ADC value were of great predictive value inefficacy of chemoradiotherapy in NPC patients.

Keywords: Diffusion-weighted magnetic resonance imaging, nasopharyngeal carcinoma, lymph node, apparent diffusion coefficient, receiver operating characteristic curve, region of interests, chemoradiotherapy, efficiency

Introduction

Nasopharyngeal carcinoma (NPC), a globally common malignant tumor, originating from the epithelium of the nasopharynx, which is highly malignant with early distant metastasis and local invasion, presents a special geographic and racial distribution [1, 2]. As an endemic disease, it is enormously more common in certain regions of Southeast Asia than elsewhere, especially occurs in South China, Cantonese region around Guangzhou, with an incidence of approximately 100-fold higher than North America and Europe [3]. NPC carcinogenesis is a multi-step procedure including many possible risk factors, and genetic susceptibility, environment factors and Epstein-Barr virus (EBV) infec-

tion were widely accepted as three major factors involved [2]. According to the World Health Organization, NPC can be classified into three categories, including squamous cell carcinoma (type 1), non-keratinizing carcinoma (type 2), and undifferentiated carcinoma (type 3) [4]. Patients with NPC usually emerge with many local symptoms, such as a blocked nose, epistaxis, otalgia, hearing loss, cranial nerve (CN), headache, distant metastasis as well as cervical lymph node metastasis [5, 6]. Treatment method for NPC patients mainly relied on the traditional radiation therapy which however is easy to result in high rate of locoregional recurrence by the complex anatomic structure of nasopharynx, while it also reported that this complex structure can be seen via imaging

examination [7, 8]. Therefore, imaging examination plays a crucial role in diagnosing of NPC.

In recent years, several magnetic resonance imaging (MRI) techniques, together with conventional methods, are being used for routine radiodiagnostic applications [9]. Diffusion-weighted magnetic resonance imaging (DW-MRI), an emerging non-invasive MRI technique, can reveal the microstructural characteristics of a tumor indirectly by inspecting the diffusive state of water molecules in viable tissue [10]. In general, DW-MRI allows a quantitative evaluation by assessing apparent diffusion coefficient (ADC) values which can estimate the random motion rate of water molecules [11]. Interestingly, the ADC value relies mainly on the presence of diffusion barriers in the water microenvironment, and varies inversely with the cell density because elevated cell density restricts water molecules diffusion in the interstitial space [12, 13]. Besides, DW-MRI is promptly acquiring importance as a valuable noninvasive biomarker for detecting tumor response to therapy in a large amount of tumors as well as for the determination of tumor aggressiveness noninvasively [14]. To be specific, its role for the evaluation of cellularity and aggressiveness in renal tumors, breast tumors, hepatocellular tumors as well as soft tissue sarcomas has been clarified [15-17]. As for its valuable efficacy on large varieties of tumors, we conducted this study to investigate the predictive value of DW-MRI and ADC values in cervical lymph node metastasis from NPC after chemoradiotherapy.

Materials and methods

Ethics statement

The study was carried out with the permission of the Institutional Review Board of the First Affiliated Hospital of Xinxiang Medical University. Written informed consents were obtained from all participants. Ethical approval for this study conformed to the standards of the Declaration of Helsinki [18].

Study subjects

Between March 2010 and January 2013, 81 patients diagnosed with nasopharyngeal carcinoma (NPC) treated in our hospital. Among 81 NPC patients, 4 patients had their treatment discontinued as a result of poor family, and 6

patients failed to complete the 5 magnetic resonance imaging (MRI) monitoring (before chemotherapy, at the end of chemotherapy, 2 weeks after radiotherapy, 4 weeks after radiotherapy, and at the end of radiotherapy). In fact, 71 NPC patients (56 males and 15 females) aged 18~70 (mean age: 49.70 ± 8.59) were randomly selected in our study. Pathological finding of biopsy showed that 50 patients (70.42%) were diagnosed with differentiated non-keratinizing carcinoma, and the rest of 21 patients (29.58%) were diagnosed with undifferentiated non-keratinizing carcinoma. All patients received relevant examinations to eliminate distant metastasis and to ascertain the staging of NPC [19]: 5 cases (7.04%) in stage T1, 35 cases (49.30%) in stage T2, 19 cases (26.76%) in stage T3, and 12 cases (16.90%) in stage T4.

The inclusion criteria were: (1) patients were diagnosed with NPC between March 2010 and January 2013, and neoplasms were confirmed from epithelia by biopsy of nasopharyngoscope; (2) patients received normal chemoradiotherapy at oncology department in our hospital; (3) patients underwent examinations before treatment, under treatment and after treatment (after routine treatment). The examinations before treatment included conventional plain scan and sequence, and patients who weren't contraindicated to the enhancement scanning, such as having allergy history of nuclear magnetic enhancement contrast agent injection and allergic constitution, were underwent dynamic contrast-enhanced scan after the end of plain scan or at the next day. Besides, the exclusion criteria were: (1) neoplasms were not originated from epithelia; (2) patients with contraindications or failed to complete relevant examinations on time; (3) patients received other treatments by the reason of other cancers before examinations; (4) patients failed to complete 6 times MRI monitoring; (5) patients aged >70 years old, or patients with severe cardiovascular diseases or respiratory diseases.

The inclusion criteria of enrolled cervical lymph node metastasis before chemoradiotherapy according to the MRI diagnostic criteria of NPC staging revised in 2008 [20]: (1) cross section film presented the minimum diameter of lymph node ≥ 10 mm; (2) necrosis in center or ring-enhancement; (3) with 3 or more than 3 lymph nodes in the same high-risk area, which a minimum diameter of the maximum cross section

≥8 mm (high-risk area: N₀, II area; N+, the next area of the area where the lymph nodes are located); (4) extracapsular invasion of lymph node: a) irregular enhancement in the edge of lymph; b) partial or entire disappear of space of surrounding fat; c) lymph node was amalgamation mutually; (5) retropharyngeal lymph node: minimum diameter of the maximum cross section ≥5 mm. According to this criterion, a sum of 251 lymph nodes was diagnosed as metastatic lymph nodes by MRI before treatment.

Treatment and therapeutic evaluation

All patients were treated with two cycles of chemotherapy, and then treated within intensity modulated radiation therapy (IMRT). At the 1~3 days, cis-platinum complexes chemotherapy (40 mg/m²) was conducted, and a 21-days pause was needed during two chemotherapies. Radiation therapy was conducted under a total dose between 65~70 Gy in 6 weeks (30 times).

World Health Organization (WHO) proposes a common view on efficacy assessments of chemoradiotherapy in tumors via measuring of the area of lymph nodes (product of the longest diameter and vertical shortest diameter) [21]. The evaluation criterion was: (1) complete response (CR): focus disappeared; (2) partial response (PR): lymph node was reduced more than 50%; (3) no change (NC): lymph node was reduced less than 50% or increased no more than 25%; (4) progressive disease (PD): lymph node was increased about 25% or more, or a new lymph node was discovered. Because of the low number of NC and PD groups, PR, NC and PD groups were combined and analyzed as non CR group.

MRI method

All patients received conventional MRI and diffusion-weighted imaging (DWI) examinations in nasopharynx and neck at the following five times: before chemotherapy, at the end of chemotherapy, 2 weeks after radiotherapy, 4 weeks after radiotherapy, and at the end of radiotherapy.

Philips Achieva (Best, Netherlands) MR scanner imaging system was used in all examinations. All patients were received MR plain scan, dynamic contrast-enhanced scan and MRI. (1) MRI imaging parameters were as follows: axial

spin-echo (SE) T1-weighted imaging (T1WI) sequence: Repetition Time (TR), 509 ms/Excitation Time (TE), 14 ms; slice thickness, 4 mm/slice gap, 1.2 mm; number of slices, 30~40; number of excitations (NEX), 4; field of view (FOV), 23~30×23~30 cm; matrix, 256×256; axial turbo spin-echo (TSE) T2WI sequence: TR, 9360 ms/TE, 99 ms; time to inversion (TI), 120 ms; slice thickness, 4 mm/slice gap, 1.2 mm; number of slices, 30~40; NEX, 4; field of view (FOV), 23~30×23~30 cm; matrix, 256×256; coronal TSE T2WI sequence: slice thickness, 4 mm/gap, 1.2 mm; number of slices, 15~20 (the other parameters were the same as axial TSE T2WI sequence). (2) Enhanced-T1 high resolution isotropic volume excitation (e-THRIVE) sequence was applied in dynamic contrast-enhanced scan, while, gadolinium injection of acid was used as contrast agent. The contrast agent was injected into forearm vein with a speed of 2 ml/s by a high pressure injector (Total amount according to 0.1 mmol/kg weight). And then, 0.9% sodium chloride (20 ml) was injected at the same speed with contrast agent to wash catheter. Before the injection of contrast agent, the scanning was conducted, and the contrast agent was injected after the scanning for 40 s. The scanning was conducted for 8 times continuously. (3) Single shot echo planar technique was applied in DWI. DWI imaging parameters were as follows: TR, 3800 ms/TE, 93 ms; TI, 2500 ms; slice thickness, 5 mm/slice gap, 1.5 mm; NSL, 20; FOV, 24 cm; NEX, 1; scanning time, 74 s; b value, 0/800 s/mm². After scanning, all the data were uploaded into work station for image postprocessing.

Region of interest (ROI) was delineated in the ADC fused image under the combination of conventional MRI and DWI. During delineation, we need to try best to include the substantial region of tumor, avoid necrotic and cystic changes. After delineation, the ADC values were measured, and the ADC values of the maximum cross-sectional area and lymph nodes at the upper and lower 2-3 levels were collected for calculating the mean values, and the appreciation and appreciation rate of ADC values in different time periods. The formulas of calculating appreciation and appreciation rate of ADC values were [22]: $\Delta\text{ADC} = \text{post-ADC value} - \text{pre-ADC value}$; $\%\Delta\text{ADC} = (\text{the second ADC value} - \text{the first ADC value}) / \text{ADC value}$

DW-MRI and NPC after chemoradiotherapy

Table 1. Baseline characteristics of patients with nasopharyngeal darcinoma (NPC)

	CR group	Non-CR group	P
Age	49.13±8.58	51.05±8.66	0.394
Gender			
Male	41	15	0.319
Female	9	6	
Smoking			
Yes	14	5	0.716
No	36	16	
Drinking			
Yes	9	3	0.703
No	41	18	
Family history of tumor			
Yes	6	3	0.792
No	44	18	
Size of lymph node			
≤10 mm	10	5	0.720
>10 mm	40	16	
Pathological type			
Differentiation	36	14	0.653
Undifferentiation	14	7	
Clinical stages			
T1	4	1	0.021
T2	28	7	
T3	14	5	
T4	4	8	

NPC: nasopharyngeal darcinoma.

before treatment $\times 100$. The pre-ADC value and post-ADC value means ADC values at two contiguous time points.

The maximum cross-sectional area of cervical lymph node metastasis: according to the axial T2WI imaging of nasopharynx and neck, we used a method of delineating edge to calculate sectional area of transverse view of lymph nodes. The maximum number was selected as the maximum cross-sectional area of lymph nodes, and the retreat value and retreat rate of the maximum cross-sectional area in different time periods were also calculated. The formulas of calculating retreat value and retreat rate of ADC values were [22]: $\Delta S = \text{post-S} - \text{pre-S}$; $\% \Delta S = (\text{post-S} - \text{pre-S}) / \text{pre-S} \times 100$. The pre-S and post-S means the maximum cross-sectional area of lymph node at two contiguous time points, and S before treatment means the maximum cross-sectional area of lymph node before treatment.

Statistical analysis

SPSS 21.0 software (SPSS Inc, Chicago, IL, USA) was used for data analyzing. Continuous data were presented with mean \pm standard deviation ($\bar{X} \pm s$) and tested by Student's *t* test. Categorical data were measured by χ^2 test and presented by percentage. Receiver operating characteristic curve (ROC) was conducted to calculate ADC values to predict the threshold value and efficacy of CR group after treatment. A *P* value of less than 0.05 was considered to be statistically significant.

Results

Baseline characteristics

The exact numbers of each group were: 50 cases in CR group (70.42%, 50/71), 19 cases in PR group (26.76%, 19/71), 1 case in NC group (1.41%, 1/71) and 1 case in PD group (1.41%, 1/71). Because of the low number of NC and PD groups, PR, NC and PD groups were combined and analyzed as non-CR group (21 cases, 29.58%, 21/71). A significant difference was found in clinical stages between two groups (*P* = 0.021), while, no such difference was observed in other characteristics (all *P* > 0.05) (Table 1).

Changes of metastatic lymph nodes on conventional MRI, DWI and ADC images before and after treatment

Before treatment, metastatic lymph nodes showed isointense on T1WI and hyperintense on T2WI, hyperintense on DWI images (part of the larger lymph node central necrosis showed hypointense); metastatic lymph nodes showed hypointense on ADC images (part of the larger lymph node central necrosis showed hyperintense). At the end of treatment, significantly reduced lymph node size, decreased intensity on T2WI and DWI, and increased intensity on ADC images were observed (Figure 1).

The maximum cross-sectional area of metastatic lymph nodes before and after treatment

During the chemoradiotherapy, the maximum cross-sectional area of metastatic lymph nodes in both CR and non-CR group were reduced (Figure 2). The maximum cross-sectional area

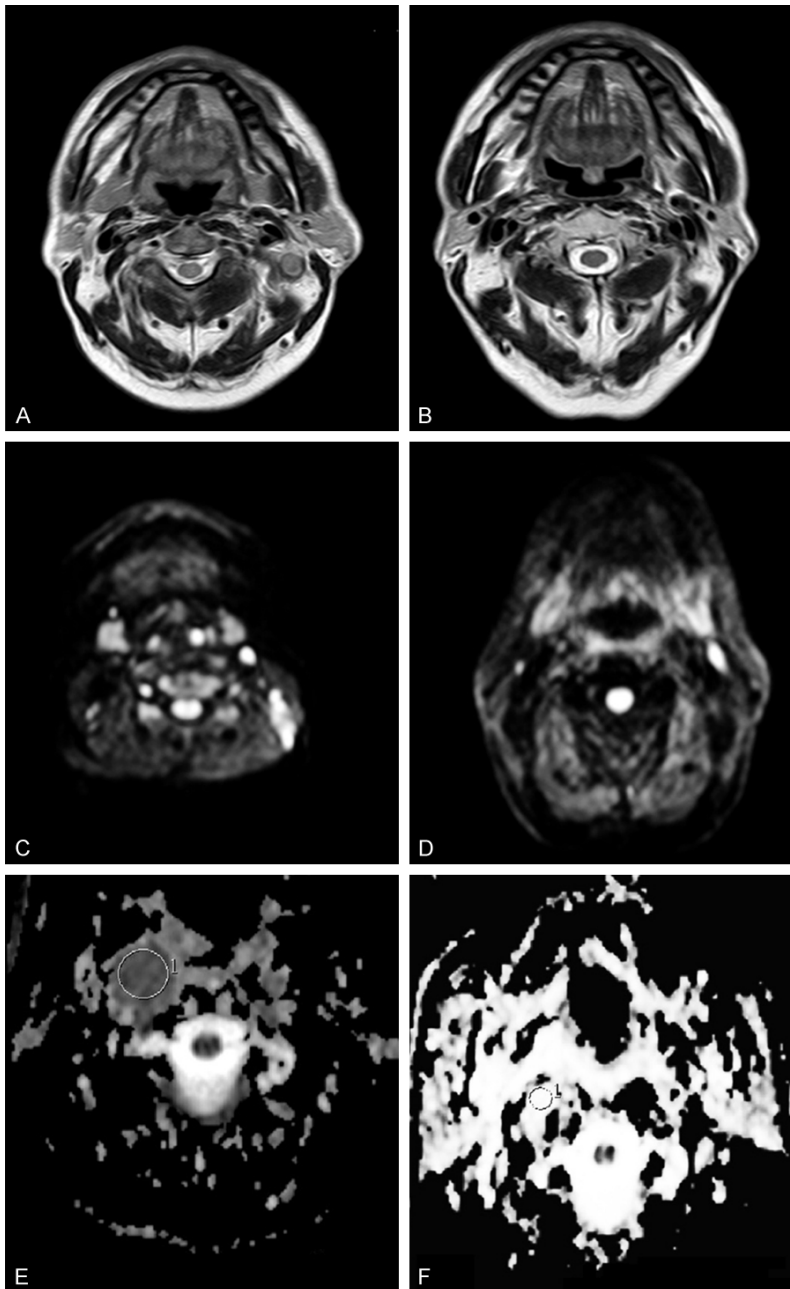


Figure 1. T2WI, DWI and ADC images of metastatic lymph nodes of nasopharyngeal carcinoma before and after treatment (A: T2WI image before treatment; B: T2WI image after treatment; C: DWI image before treatment; D: DWI image after treatment; E: ADC image before treatment; F: ADC image after treatment).

of metastatic lymph nodes in CR group was $245.75 \pm 188.64 \text{ mm}^2$ before treatment, while, it changed into $88.32 \pm 82.76 \text{ mm}^2$ after treatment. Significant differences were found in comparison of the maximum cross-sectional area before and after treatment ($t = 9.952$, $P < 0.001$) and the contiguous time points (all $P < 0.05$) (Table 2). In CR group, among those four time periods, a significant difference was

found in the retreat values of the maximum cross-sectional area between $\Delta S_{\text{after chemotherapy}}$ and $\Delta S_{\text{2 weeks of radiotherapy}}$ (all $P < 0.05$); nevertheless, there was no statistical difference between other time periods (all $P > 0.05$). Besides, no significant difference was found in retreat rates in contiguous time points (all $P > 0.05$). As for the non-CR group, no significant difference was found in the maximum cross-sectional area of metastatic lymph nodes before and after treatment (before: $247.96 \pm 189.72 \text{ mm}^2$; after: $89.25 \pm 83.69 \text{ mm}^2$; $t = 7.306$, $P < 0.001$). Significant differences were found in comparison of the maximum cross-sectional area before and after chemotherapy ($t = 2.548$, $P = 0.013$), while, no such differences were observed in other time periods. No such differences were observed in retreat values in contiguous time points in non-CR group (all $P > 0.05$). In addition, no significant difference was also found in retreat rates in contiguous time points (all $P > 0.05$) (Table 2).

The ADC values of metastatic lymph nodes before and after treatment

The mean ADC values of metastatic lymph nodes presented an increasing

trend during chemoradiotherapy (Figure 3). The ADC values of metastatic lymph nodes in CR group before and after treatment showed $(7.72 \pm 1.24) \times 10^{-4} \text{ mm}^2/\text{s}$ and $(14.56 \pm 2.33) \times 10^{-4} \text{ mm}^2/\text{s}$, respectively. Significant differences were found in the comparison of the ADC value between before and after treatment ($t = 34.62$, $P < 0.001$), and other contiguous time points (all $P < 0.05$) except the comparison between ADC_4

DW-MRI and NPC after chemoradiotherapy

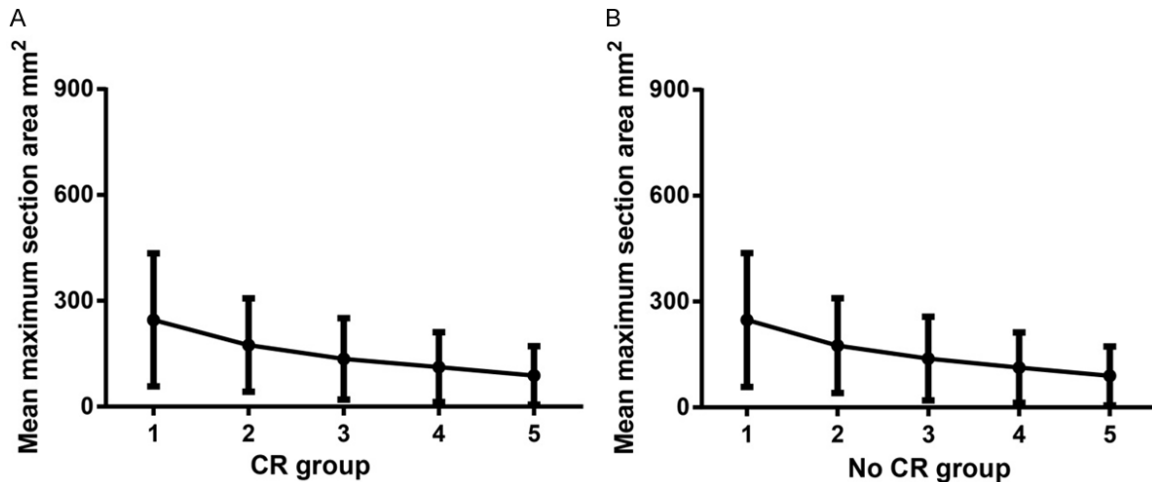


Figure 2. Curves (mm²) of the maximum cross-sectional area of metastatic lymph nodes among all mentioned time points during treatment (A: Complete response [CR] group, the five numbers in horizontal ordinate represent for the five time points: before chemotherapy, at the end of chemotherapy, 2 weeks of radiotherapy, 4 weeks of radiotherapy, at the end of radiotherapy, respectively; B: Non-CR group, the five numbers in horizontal ordinate represent for the five time points: before chemotherapy, at the end of chemotherapy, 2 weeks of radiotherapy, 4 weeks of radiotherapy, at the end of radiotherapy, respectively).

Table 2. The maximum cross-sectional area of metastatic lymph nodes incomplete response (CR) group and non-CR group during chemoradiotherapy at different time points (mm²)

	CR group	non-CR group	t1	P1	t2	P2
S _{before chemoradiotherapy}	245.75±188.64	247.96±189.72	4.100 ^a	<0.001 ^a	2.548 ^a	0.013 ^a
S _{after chemoradiotherapy}	174.59±132.58	175.34±134.18	2.776 ^b	0.006 ^b	1.917 ^b	0.059 ^b
S _{2 weeks after radiotherapy}	135.48±115.63	138.51±118.31	2.030 ^c	0.044 ^c	1.676 ^c	0.159 ^c
S _{4 weeks after radiotherapy}	111.95±98.85	113.19±99.78	2.389 ^d	0.018 ^d	1.422 ^d	0.098 ^d
S _{after radiotherapy}	88.32±82.76	89.25±83.69	9.952 ^e	<0.001 ^e	7.306 ^e	<0.001 ^e
ΔS _{before-after chemotherapy}	71.16±97.23	72.63±78.13	2.016 ^f	0.049 ^f	1.183 ^f	0.074 ^f
ΔS _{after chemotherapy-2 weeks after radiotherapy}	39.11±46.87	41.16±48.88	1.931 ^g	0.059 ^g	1.263 ^g	0.221 ^g
ΔS _{2-4 weeks of radiotherapy}	23.53±25.54	25.32±27.34	0.903 ^h	0.903 ^h	0.138 ^h	0.891 ^h
ΔS _{4 weeks of radiotherapy to the end of radiotherapy}	22.93±27.99	23.94±28.76				
%ΔS _{after chemotherapy}	28.96±23.25	29.29±24.45	1.317 ⁱ	0.194 ⁱ	0.711 ⁱ	0.485 ⁱ
%ΔS _{2 weeks after radiotherapy}	22.40±23.46	23.47±24.53	1.305 ^j	0.198 ^j	0.956 ^j	0.350 ^j
%ΔS _{2-4 weeks of radiotherapy}	17.37±14.95	18.28±15.65	0.889 ^k	0.378 ^k	0.447 ^k	0.660 ^k
%ΔS _{4 weeks of radiotherapy to the end of radiotherapy}	20.48±20.20	21.15±21.18				

t1 and P1: comparison results in the CR group at different time points; t2 and P2: comparison results in the non-CR group at different time points; a~e: comparison of S (a: before chemoradiotherapy vs. after chemoradiotherapy; b: after chemoradiotherapy vs. 2 weeks after radiotherapy; c: 2 weeks after radiotherapy vs. 4 weeks after radiotherapy; d: 4 weeks after radiotherapy vs. after radiotherapy; e: before chemoradiotherapy vs. after radiotherapy); f~h: comparison of ΔS (f: before-after chemotherapy vs. after chemotherapy-2 weeks after radiotherapy; g: after chemotherapy-2 weeks after radiotherapy vs. 2-4 weeks of radiotherapy; h: 2-4 weeks of radiotherapy vs. 4 weeks of radiotherapy to the end of radiotherapy); i~k: comparison of %ΔS (i: before-after chemotherapy vs. after chemotherapy-2 weeks after radiotherapy; j: after chemotherapy-2 weeks after radiotherapy vs. 2-4 weeks of radiotherapy; k: 2-4 weeks of radiotherapy vs. 4 weeks of radiotherapy to the end of radiotherapy).

and ADC_{after radiotherapy} (t = 1.616, P = 0.108 > 0.05) (Table 3). The appreciation of ADC values in the above four time points suggesting statistically significant differences (all P < 0.05). Similarly, no significant difference was

found between %ΔADC_{after chemotherapy} and %ΔADC_{2 weeks of radiotherapy} (P > 0.05); nevertheless, a significant difference was observed in other two contiguous time points (all P < 0.05). With regard to the non-CR group, compared to the

DW-MRI and NPC after chemoradiotherapy

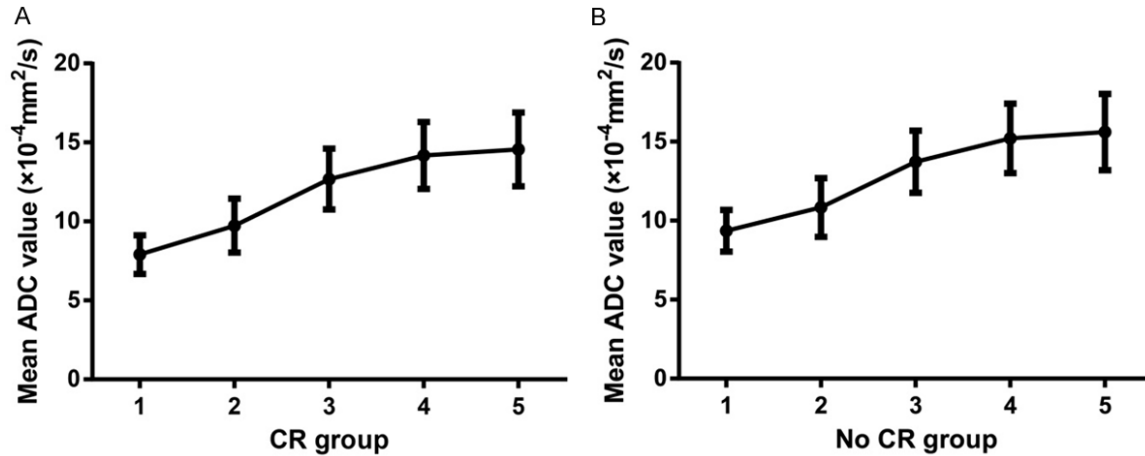


Figure 3. Curves of mean apparent diffusion coefficient (ADC) values ($\times 10^{-4}$ mm²/s) among all mentioned time points during treatment (A: Complete response [CR] group, the five numbers in horizontal ordinate represent for the five time points: before chemotherapy, at the end of chemotherapy, 2 weeks of radiotherapy, 4 weeks of radiotherapy, at the end of radiotherapy, respectively; B: Non-CR group, the five numbers in horizontal ordinate represent for the five time points: before chemotherapy, after chemotherapy, 2 weeks of radiotherapy, 4 weeks of radiotherapy, after radiotherapy, respectively).

Table 3. The apparent diffusion coefficient (ADC) of metastatic lymph nodes incomplete response (CR) group and non-CR group during chemoradiotherapy at different time points ($\times 10^{-4}$ mm²/s)

	CR group	non-CR group	t1	P1	t2	P2
ADC _{before chemoradiotherapy}	7.72±1.24	9.36±1.32	13.270 ^a	<0.001 ^a	5.829 ^a	<0.001 ^a
ADC _{after chemoradiotherapy}	9.73±1.71	10.84±1.86	14.580 ^b	<0.001 ^b	9.339 ^b	<0.001 ^b
ADC _{2 weeks after radiotherapy}	12.68±1.92	13.72±1.97	7.134 ^c	<0.001 ^c	4.348 ^c	<0.001 ^c
ADC _{4 weeks after radiotherapy}	14.18±2.12	15.21±2.20	7.134 ^c	0.108 ^d	1.147 ^d	0.255 ^d
ADC _{after radiotherapy}	14.56±2.33	15.61±2.41	34.620 ^e	<0.001 ^e	20.37 ^e	<0.001 ^e
Δ ADC _{before-after chemotherapy}	2.01±1.56	1.48±1.06	2.687 ^f	0.010 ^f	3.327 ^f	0.003 ^f
Δ ADC _{after chemotherapy-2 weeks after radiotherapy}	2.95±1.87	2.88±1.79	4.022 ^g	0.001 ^g	3.566 ^g	0.002 ^g
Δ ADC _{2-4 weeks of radiotherapy}	1.50±1.71	1.49±1.70	3.623 ^h	0.001 ^h	2.66 ^h	0.015 ^h
Δ ADC _{4 weeks of radiotherapy to the end of radiotherapy}	0.38±1.65	0.40±1.67				
% Δ ADC _{after chemotherapy}	26.04±20.86	15.81±10.36	1.096 ⁱ	0.278 ⁱ	2.748 ⁱ	0.012 ⁱ
% Δ ADC _{2 weeks after radiotherapy}	30.32±17.73	26.57±12.83	6.683 ^j	<0.001 ^j	4.937 ^j	<0.001 ^j
% Δ ADC _{2-4 weeks of radiotherapy}	11.83±14.28	10.86±13.28	2.785 ^k	0.008 ^k	1.505 ^k	0.148 ^k
% Δ ADC _{4 weeks of radiotherapy to the end of radiotherapy}	2.70±17.49	2.63±16.28				

t1 and P1: comparison results in the CR group at different time points; t2 and P2: comparison results in the non-CR group at different time points; a~e: comparison of ADC values (a: before chemoradiotherapy vs. after chemoradiotherapy; b: after chemoradiotherapy vs. 2 weeks after radiotherapy; c: 2 weeks after radiotherapy vs. 4 weeks after radiotherapy; d: 4 weeks after radiotherapy vs. after radiotherapy; e: before chemoradiotherapy vs. after radiotherapy); f~h: comparison of Δ ADC values (f: before-after chemotherapy vs. after chemotherapy-2 weeks after radiotherapy; g: after chemotherapy-2 weeks after radiotherapy vs. 2-4 weeks of radiotherapy; h: 2-4 weeks of radiotherapy vs. 4 weeks of radiotherapy to the end of radiotherapy); i~k: comparison of % Δ ADC values (i: before-after chemotherapy vs. after chemotherapy-2 weeks after radiotherapy; j: after chemotherapy-2 weeks after radiotherapy vs. 2-4 weeks of radiotherapy; k: 2-4 weeks of radiotherapy vs. 4 weeks of radiotherapy to the end of radiotherapy).

ADC value of metastatic lymph nodes before treatment ($[9.36\pm 1.32]\times 10^{-4}$ mm²/s), the ADC value of metastatic lymph nodes after treatment ($[16.61\pm 2.41]\times 10^{-4}$ mm²/s) had an elevated number, indicating statistical significance

($t = 20.37, P < 0.001$). **Table 3** revealed that statistical difference in all the contiguous time points (all $P < 0.05$) except the comparison between ADC_{4 weeks of radiotherapy} and ADC_{after radiotherapy} ($t = 1.147, P = 0.225$). The appreciation of the

DW-MRI and NPC after chemoradiotherapy

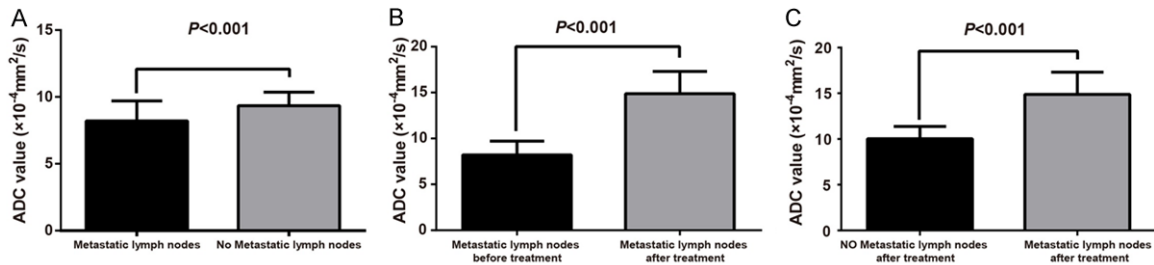


Figure 4. Comparison of mean apparent diffusion coefficient (ADC) values between metastatic lymph nodes and no metastatic lymph nodes before and after treatment (A: Metastatic lymph nodes vs. no metastatic lymph nodes before treatment; B: Metastatic lymph nodes before treatment vs. no metastatic lymph nodes after treatment; C: Metastatic lymph nodes vs. no metastatic lymph nodes after treatment).

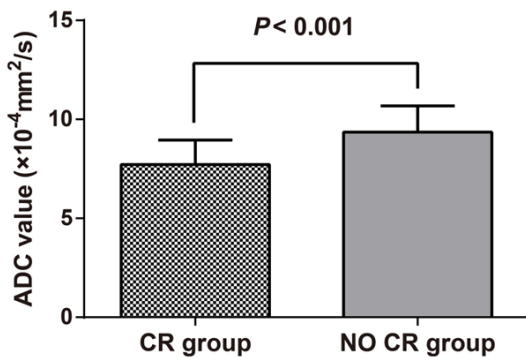


Figure 5. Comparison of mean apparent diffusion coefficient (ADC) values before treatment between complete response (CR) and non-CR group.

ADC values during treatment in non-CR group suggesting statistically significant differences (all $P < 0.05$). Besides, a statistical difference was found in the comparison of the appreciation rates of the ADC values between $\% \Delta \text{ADC}_{\text{after chemotherapy}}$ and $\% \Delta \text{ADC}_{2 \text{ weeks of radiotherapy}}$ (all $P < 0.05$), while, no such difference was found between $\% \Delta \text{ADC}_{2-4 \text{ weeks of radiotherapy}}$ and $\% \Delta \text{ADC}_{4 \text{ weeks of radiotherapy to the end of radiotherapy}}$ ($P > 0.05$) (Table 3).

Comparison of mean ADC values between metastatic lymph nodes and no metastatic lymph nodes

Compared to the ADC value of metastatic lymph nodes before treatment ($[8.21 \pm 1.47] \times 10^{-4} \text{ mm}^2/\text{s}$), the ADC value of no metastatic lymph nodes before treatment ($[9.34 \pm 1.01] \times 10^{-4} \text{ mm}^2/\text{s}$) increased statistically significantly ($t = 5.110$, $P < 0.001$). An obviously increasing trend was found in the mean ADC values of residual lymph nodes one month after treatment ($[14.87 \pm 2.40] \times 10^{-4} \text{ mm}^2/\text{s}$) compared with those before treatment and no metastatic

lymph nodes after treatment ($[10.02 \pm 1.38] \times 10^{-4} \text{ mm}^2/\text{s}$), which indicated statistical significances (residual lymph nodes one month after treatment vs. residual lymph nodes before treatment: $t = 19.49$, $P < 0.001$; residual lymph nodes one month after treatment vs. no metastatic lymph nodes: $t = 14.97$, $P < 0.001$) (Figure 4).

Comparison of ADC values between CR and non-CR group, and ROC analysis

The ADC value in CR group before treatment ($[7.72 \pm 1.24] \times 10^{-4} \text{ mm}^2/\text{s}$) was lower than that in non-CR group ($[9.36 \pm 1.32] \times 10^{-4} \text{ mm}^2/\text{s}$), which expressed statistical significance ($P < 0.001$) (Figure 5). The sensitivity, specificity, positive predictive value, negative predictive value, accuracy and area under curve (AUC) after treatment of NPC were predicted by the threshold value setting by mean ADC value before treatment ($8.11 \times 10^{-4} \text{ mm}^2/\text{s}$). Besides, the exact numbers of the above data were: 0.905, 0.680, 0.763, 0.583, 0.732 and 0.816 ($P < 0.001$, 95% confidence interval (CI): 0.708~0.925) (Figure 6).

Discussion

In the present study, we applied DWI sequences together with the standard MRI technique to determine the utility of DW-MRI and ADC values in cervical lymph node metastasis from NPC after chemoradiotherapy. The main achievement of our study was proved the predictive role of DW-MRI and ADC values in NPC after chemoradiotherapy, and provided an evidence for studying other tumors.

NPC originates from a hidden anatomical site, and is more closely associated with advanced clinical stage with higher incidence of invasion

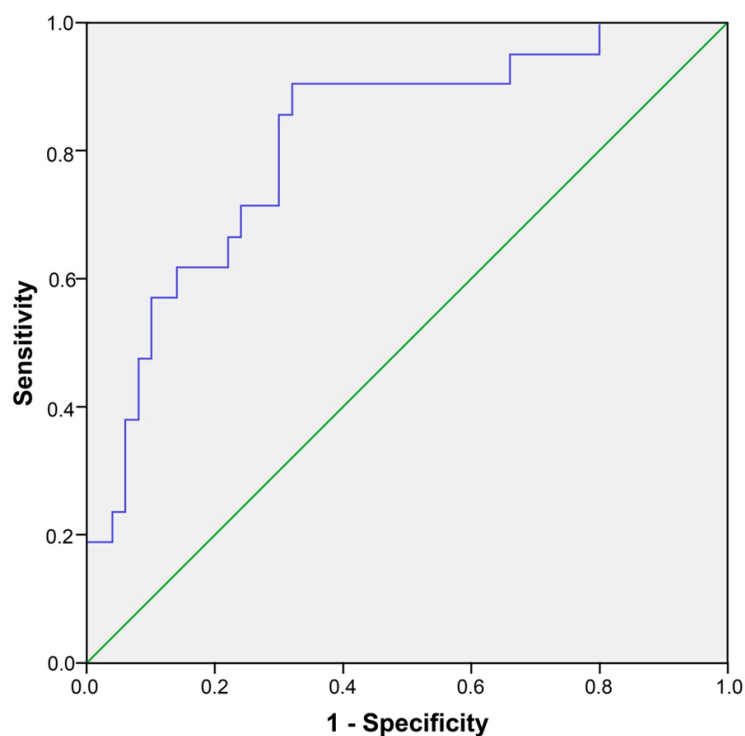


Figure 6. Receiver operating characteristic curve (ROC) of the prediction after treatment by apparent diffusion coefficient (ADC) values before treatment.

and metastasis at the time of diagnosis [2]. The treatment of early NPC mainly depends on the combination of radiotherapy and chemotherapy, but the remaining tumor tissues still can be found among a part of patients, and cervical lymph node metastasis contained approximately 18% incidence [8, 23]. Evidence showed that the accuracy of DW-MRI detection depends on the average ADC values, which associates with tumor type and size, and has been successfully applied to malignancies diagnosis and early detection in tumor recurrence [24]. Also, effective anti-tumor therapy can lead to dissolution of tumor cells and increasing width of cell gap to enhance the diffusion ability of water molecules, and then resulted in the increasing ADC value rapidly, while, the decreased ADC value of the lesion compared with those before treatment presented a bad effect [25]. Furthermore, a large number of domestic and foreign studies showed that the ADC value of the vast majority of malignant tumors is significantly lower than that of benign tumors; moreover, the lower degree of differentiation of the tumor may correlated with the lower ADC value [26, 27]. Reductions, resulting in an increased hypercellularity and nuclear-to-

cytoplasmic ratio in both the diffusion space and the extracellular matrix of the water protons in the extracellular and intracellular dimensions have been deemed as potential reasons for the decreased ADC values within malign at lesions compared with nonmalignant tissue [28]. In our study, an increasing trend of ADC value of metastatic lymph nodes was also observed during chemoradiotherapy. To be specific, after the evaluation of efficacy of chemoradiotherapy, the higher ADC values of metastatic lymph nodes in CR group after treatment was also found compared to those before treatment. Consistent with our results, *Perrone et al.* also proved a lower ADC value of metastatic lymph nodes under the circumstance of cervical lymph node metastasis from NPC [29]. Likewise, in our study, metastatic lymph nodes had evidently lower ADC values than

no metastatic lymph nodes; this finding corroborated the results of prior investigators [30, 31].

Besides, we also found that the maximum cross-sectional area of cervical lymph node metastasis from NPC presented a continuously retreat trend during chemoradiotherapy. In the presented study, we applied a method of delineating edge to calculate sectional area of transverse view of lymph nodes. A strong relationship was proved among tumor volume, local control rate, and survival rate [32]. Besides, tumors with large volumes frequently contained more clonogenic tumor cells, and greater tumor burden usually need larger doses of radiation to create a radical cure [33]. In addition, as previously described by *Qi et al.*, the tumor size presented by DW-MRI was most close to surgical pathology, thereby, the utilization of DW-MRI can more accurately delineate the target area of NPC, and to reduce the damage of brain tissue basically [34]. In our study, radiation therapy was conducted an image delineated by DW-MRI with a total dose between 65~70 Gy in 6 weeks (30 times), which can better reduce the maximum cross-sectional area of cervical lymph node metastasis from NPC.

To sum up, our study proved compelling evidence that both DW-MRI and ADC value were of great predictive value in efficacy of chemoradiotherapy in NPC patients which provides evidence for clinical individual and studying of other cancers. However, it should be noted that the limited sample size of our study needs to be further investigated and confirmed.

Acknowledgements

We would like to give our sincere appreciation to the reviewers for their helpful comments on this article.

Disclosure of conflict of interest

None.

Address correspondence to: Dongming Han, Department of Medical Imaging, The First Affiliated Hospital of Xixiang Medical University, No. 88, Jiankang Road, Weihui 453100, P.R. China. Tel: +86-0373-44047310; Fax: +86-0373-44047310; E-mail: handongming_han@yeah.net

References

- [1] Arnold M, Wildeman MA, Visser O, Karim-Kos HE, Middeldorp JM, Fles R, Bing Tan I, Coebergh JW. Lower mortality from nasopharyngeal cancer in The Netherlands since 1970 with differential incidence trends in histopathology. *Oral Oncol* 2013; 49: 237-243.
- [2] Wu Z, Weng D, Li G. Quantitative proteome analysis of overexpressed Cripto-1 tumor cell reveals 14-3-3gamma as a novel biomarker in nasopharyngeal carcinoma. *J Proteomics* 2013; 83: 26-36.
- [3] Nie Y, Liu X, Qu S, Song E, Zou H, Gong C. Long non-coding RNA HOTAIR is an independent prognostic marker for nasopharyngeal carcinoma progression and survival. *Cancer Sci* 2013; 104: 458-464.
- [4] Yoshizaki T, Ito M, Murono S, Wakisaka N, Kondo S, Endo K. Current understanding and management of nasopharyngeal carcinoma. *Auris Nasus Larynx* 2012; 39: 137-144.
- [5] Chong VF, Ong CK. Nasopharyngeal carcinoma. *Eur J Radiol* 2008; 66: 437-447.
- [6] King AD, Bhatia KS. Magnetic resonance imaging staging of nasopharyngeal carcinoma in the head and neck. *World J Radiol* 2010; 2: 159-165.
- [7] Huang CD, Tang MZ. [Progress of treating nasopharyngeal carcinoma by Chinese pharmacy and radiotherapy]. *Zhongguo Zhong Xi Yi Jie He Za Zhi* 2013; 33: 1575-1578.
- [8] Lin YH, Chang KP, Lin YS, Chang TS. Evaluation of effect of body mass index and weight loss on survival of patients with nasopharyngeal carcinoma treated with intensity-modulated radiation therapy. *Radiat Oncol* 2015; 10: 136.
- [9] Avcu S, Koseoglu MN, Ceylan K, Bulut MD, Unal O. The value of diffusion-weighted MRI in the diagnosis of malignant and benign urinary bladder lesions. *Br J Radiol* 2011; 84: 875-882.
- [10] Hong J, Yao Y, Zhang Y, Tang T, Zhang H, Bao D, Chen Y, Pan J. Value of magnetic resonance diffusion-weighted imaging for the prediction of radiosensitivity in nasopharyngeal carcinoma. *Otolaryngol Head Neck Surg* 2013; 149: 707-713.
- [11] Kierans AS, Bennett GL, Mussi TC, Babb JS, Rusinek H, Melamed J, Rosenkrantz AB. Characterization of malignancy of adnexal lesions using ADC entropy: comparison with mean ADC and qualitative DWI assessment. *J Magn Reson Imaging* 2013; 37: 164-171.
- [12] Sun YS, Cui Y, Tang L, Qi LP, Wang N, Zhang XY, Cao K, Zhang XP. Early evaluation of cancer response by a new functional biomarker: apparent diffusion coefficient. *AJR Am J Roentgenol* 2011; 197: W23-29.
- [13] Ginat DT, Mangla R, Yeane G, Johnson M, Ekholm S. Diffusion-weighted imaging for differentiating benign from malignant skull lesions and correlation with cell density. *AJR Am J Roentgenol* 2012; 198: W597-601.
- [14] Harry VN, Semple SI, Parkin DE, Gilbert FJ. Use of new imaging techniques to predict tumour response to therapy. *Lancet Oncol* 2010; 11: 92-102.
- [15] Muhi A, Ichikawa T, Motosugi U, Sano K, Matsuda M, Kitamura T, Nakazawa T, Araki T. High-b-value diffusion-weighted MR imaging of hepatocellular lesions: estimation of grade of malignancy of hepatocellular carcinoma. *J Magn Reson Imaging* 2009; 30: 1005-1011.
- [16] Costantini M, Belli P, Rinaldi P, Bufi E, Giardina G, Franceschini G, Petrone G, Bonomo L. Diffusion-weighted imaging in breast cancer: relationship between apparent diffusion coefficient and tumour aggressiveness. *Clin Radiol* 2010; 65: 1005-1012.
- [17] Schnapauff D, Zeile M, Niederhagen MB, Fleige B, Tunn PU, Hamm B, Dudeck O. Diffusion-weighted echo-planar magnetic resonance imaging for the assessment of tumor cellularity in patients with soft-tissue sarcomas. *J Magn Reson Imaging* 2009; 29: 1355-1359.
- [18] M PN. World Medical Association publishes the Revised Declaration of Helsinki. *Natl Med J India* 2014; 27: 56.

DW-MRI and NPC after chemoradiotherapy

- [19] Lee AW, Ng WT, Chan LK, Chan OS, Hung WM, Chan CC, Cheng PT, Sze H, Lam TS, Yau TK. The strength/weakness of the AJCC/UICC staging system (7th edition) for nasopharyngeal cancer and suggestions for future improvement. *Oral Oncol* 2012; 48: 1007-1013.
- [20] Lin ZX, Yang ZN, Zhan YZ, Xie WJ, Li GW, Feng HT. [Application study of the 2008 staging system of nasopharyngeal carcinoma]. *Ai Zhong* 2009; 28: 1029-1032.
- [21] Suzuki C, Jacobsson H, Hatschek T, Torkzad MR, Boden K, Eriksson-Alm Y, Berg E, Fujii H, Kubo A, Blomqvist L. Radiologic measurements of tumor response to treatment: practical approaches and limitations. *Radiographics* 2008; 28: 329-344.
- [22] Kato H, Kanematsu M, Tanaka O, Mizuta K, Aoki M, Shibata T, Yamashita T, Hirose Y, Hoshi H. Head and neck squamous cell carcinoma: usefulness of diffusion-weighted MR imaging in the prediction of a neoadjuvant therapeutic effect. *Eur Radiol* 2009; 19: 103-109.
- [23] Lee SW, Chen TJ, Lin LC, Li CF, Chen LT, Hsing CH, Hsu HP, Tsai CJ, Huang HY, Shiue YL. Overexpression of thymidylate synthetase confers an independent prognostic indicator in nasopharyngeal carcinoma. *Exp Mol Pathol* 2013; 95: 83-90.
- [24] Neubauer H, Evangelista L, Hassold N, Winkler B, Schlegel PG, Kostler H, Hahn D, Beer M. Diffusion-weighted MRI for detection and differentiation of musculoskeletal tumorous and tumor-like lesions in pediatric patients. *World J Pediatr* 2012; 8: 342-349.
- [25] Vandecaveye V, Dirix P, De Keyser F, Op de Beeck K, Vander Poorten V, Hauben E, Lambrecht M, Nuyts S, Hermans R. Diffusion-weighted magnetic resonance imaging early after chemoradiotherapy to monitor treatment response in head-and-neck squamous cell carcinoma. *Int J Radiat Oncol Biol Phys* 2012; 82: 1098-1107.
- [26] Srinivasan K, Seith Bhalla A, Sharma R, Kumar A, Roychoudhury A, Bhutia O. Diffusion-weighted imaging in the evaluation of odontogenic cysts and tumours. *Br J Radiol* 2012; 85: e864-870.
- [27] Goyal A, Sharma R, Bhalla AS, Gamanagatti S, Seth A, Iyer VK, Das P. Diffusion-weighted MRI in renal cell carcinoma: a surrogate marker for predicting nuclear grade and histological subtype. *Acta Radiol* 2012; 53: 349-358.
- [28] Srinivasan A, Dvorak R, Perni K, Rohrer S, Mukherji SK. Differentiation of benign and malignant pathology in the head and neck using 3T apparent diffusion coefficient values: early experience. *AJNR Am J Neuroradiol* 2008; 29: 40-44.
- [29] Perrone A, Guerrisi P, Izzo L, D'Angeli I, Sassi S, Mele LL, Marini M, Mazza D, Marini M. Diffusion-weighted MRI in cervical lymph nodes: differentiation between benign and malignant lesions. *Eur J Radiol* 2011; 77: 281-286.
- [30] Abdel Razek AA, Soliman NY, Elkhamary S, Alsharaway MK, Tawfik A. Role of diffusion-weighted MR imaging in cervical lymphadenopathy. *Eur Radiol* 2006; 16: 1468-1477.
- [31] Holzapfel K, Duetsch S, Fauser C, Eiber M, Rummeny EJ, Gaa J. Value of diffusion-weighted MR imaging in the differentiation between benign and malignant cervical lymph nodes. *Eur J Radiol* 2009; 72: 381-387.
- [32] Sarisahin M, Cila A, Ozyar E, Yildiz F, Turen S. Prognostic significance of tumor volume in nasopharyngeal carcinoma. *Auris Nasus Larynx* 2011; 38: 250-254.
- [33] Wu Z, Zeng RF, Su Y, Gu MF, Huang SM. Prognostic significance of tumor volume in patients with nasopharyngeal carcinoma undergoing intensity-modulated radiation therapy. *Head Neck* 2013; 35: 689-694.
- [34] Qi LP, Zhang XP, Tang L, Li J, Sun YS, Zhu GY. Using diffusion-weighted MR imaging for tumor detection in the collapsed lung: a preliminary study. *Eur Radiol* 2009; 19: 333-341.